REPORT

on EOARD grant FA8655-06-1-3048

"INFLUENCE OF DIFFERENT SOLAR DRIVERS ON THE WINDS IN THE MIDDLE ATMOSPHERE AND ON GEOMAGNETIC DISTURBANCES"

GOAL OF THE STUDY

By the term "solar activity" all types of changes in the appearance or energy output from the Sun are denoted. These changes may have different characteristics and different distribution throughout the solar cycle. Therefore, when studying the solar activity influences on terrestrial processes, we should distinguish between the different manifestations of solar activity which could have different effects on the Earth. Our study concentrates on the effects of different solar drivers on the dynamics of the atmosphere and on the disturbances caused in the geomagnetic field.

SOLAR DRIVERS

In this project, we study the effects of three types of solar drivers: solar flares, magnetic clouds as a subclass of coronal mass ejections, and high speed solar wind.

Solar flares

Historically, the first manifestations of solar activity identified as drivers of geomagnetic activity were the solar flares. A solar flare is a sudden, rapid and intense variation in the brightness of the corona caused by the explosive release of stored magnetic energy. Flares always release energy in the form of electro-magnetic radiation across the electromagnetic spectrum (from radio waves to x-rays and gamma-rays), which can be accompanied or not by energetic particles (protons and electrons), and mass flow. Even without energetic particles and mass ejection, solar flares play an important role for the ionization, chemistry changes and dynamics of the atmosphere. As the solar flares, like sunspots, are related to the solar toroidal magnetic field, they are most numerous and most intense in sunspot maximum.

Coronal mass ejections

Coronal mass ejections (CME's) are eruptions of solar plasma and embedded magnetic field from the corona. They can be associated with solar flares but can also occur independently. Coronal mass ejections are also related to the solar toroidal magnetic field, so their number and intensity are highest in sunspot maximum. CME's are considered the sources of the most intense geomagnetic storms (Gonzalez et al., 2002). However, in an earlier study (Georgieva et al., 2006) we have found that the most geoeffective solar driver are not CME's in general but magnetic clouds – a subclass of CME's distinguished by increased magnetic field intensity, low proton temperature or low plasma beta, and a smooth rotation of the magnetic field over a large angle for a period of the order of a day (Klein and Burlaga, 1980). The high magnetic field intensity and the field rotation providing prolonged period of southward magnetic field (Tsurutani et al., 1992) are the reason for the high geoeffectiveness of magnetic clouds.

REPORT DOCUMENTATION PAGE

Form Approved OMB No. 0704-0188

1. REPORT DATE *(DD-MM-YYYY)*	2. REPORT TYPE	3. DATES COVERED *(From – To)*
18-05-2007	Final Report	25 April 2006 - 16-Dec-08

4. TITLE AND SUBTITLE

Influence of different solar drivers on the winds in the middle atmosphere and on geomagnetic disturbances

5a. CONTRACT NUMBER
FA8655-06-1-3048

5b. GRANT NUMBER

5c. PROGRAM ELEMENT NUMBER

6. AUTHOR(S)

Dr. Katya Y Georgieva

5d. PROJECT NUMBER

5d. TASK NUMBER

5e. WORK UNIT NUMBER

7. PERFORMING ORGANIZATION NAME(S) AND ADDRESS(ES)
Bulgarian Academy of Sciences
Bl.3 Acad. G.Bonchev str.
Sofia 1113
Bulgaria

8. PERFORMING ORGANIZATION REPORT NUMBER

N/A

9. SPONSORING/MONITORING AGENCY NAME(S) AND ADDRESS(ES)

EOARD
Unit 4515 BOX 14
APO AE 09421

10. SPONSOR/MONITOR'S ACRONYM(S)

11. SPONSOR/MONITOR'S REPORT NUMBER(S)
Grant 06-3048

12. DISTRIBUTION/AVAILABILITY STATEMENT

Approved for public release; distribution is unlimited.

13. SUPPLEMENTARY NOTES

14. ABSTRACT

This report results from a contract tasking Bulgarian Academy of Sciences as follows: The grantee will investigate the effects of various solar drivers on the dynamics of the stratosphere and on the geomagnetic disturbances to the earth. To accomplish this, the grantee will create a database of all registered coronal mass ejections, magnetic clouds, solar flares, and high speed solar streams; neutral wind measurements at different atmospheric levels in the period of the above events; ionospheric disturbances measured at different stations worldwide;and different geomagnetic indices. In addtiona, the reaction of the neutral winds, ionospheric parameters and geomagnetic disturbances will be studied for the different solar drivers. Finally, a conclusion will be made about specific effeects of solar drivers on the middle atmopsphere..

15. SUBJECT TERMS
EOARD, Space Environment, Space Weather, Earth Sciences, Solar Physics

16. SECURITY CLASSIFICATION OF:			17. LIMITATION OF ABSTRACT	18, NUMBER OF PAGES	19a. NAME OF RESPONSIBLE PERSON
a. REPORT	b. ABSTRACT	c. THIS PAGE			GEORGE W YORK, Lt Col, USAF
UNCLAS	UNCLAS	UNCLAS	UL	27	**19b. TELEPHONE NUMBER** *(Include area code)* +44 (0)1895 616163

The direction of rotation in the magnetic clouds is not random, but is related to their solar source region: clouds originating from the northern solar hemisphere have predominantly left-handed rotation, while the ones originating from the southern solar hemisphere are predominantly right-handed, conforming to the predominant orientation of the rotating magnetic structures in the two hemispheres (Antonucci et al., 1990) On their way from the Sun to the Earth, the magnetic clouds preserve the magnetic field rotation with which they have departed from the Sun (Kumar and Rust, 1996).

The occurrence frequency of CME's as a whole is proportional to the sunspot number (Gopalswamy et al., 2003), while the occurrence frequency of magnetic clouds follows neither the sunspot cycle nor the occurrence frequency of CME's (Wu et al., 2003). The relation between CME's and magnetic clouds is still an open question. It is possible that all CME's are magnetic clouds, but they can be registered or not as magnetic clouds by satellites at the Earth's orbit depending on how favourable the satellite's trajectory is through the structure (Gopalswamy et al, 2007). Alternatively, magnetic clouds may be a special population of CME's, and if so, the question is what conditions on the Sun determine whether a CME will be a magnetic cloud or not. The relation between CME's and magnetic clouds is very important from both theoretical and practical point of view: some theories require magnetic helicity in the solar source region as a condition for the CME initiations (Nindos and Andrews, 2004), and if it can be shown that not all CME's are helical structures (that is, magnetic clouds), it would mean that these theories are not correct. If not all CME's are magnetic clouds, the understanding of whether a CME will be a magnetic cloud or not is related to the possibility to predict the probability of a CME to trigger a large geomagnetic storm.

High speed solar wind

The geomagnetic activity during the declining phase of the solar cycle can be even higher that at sunspot maximum. In this period the main drivers of terrestrial disturbances are the high speed solar wind streams originating from solar coronal holes (Gonzalez et al., 2002b). Coronal holes can live for many solar rotations, and once every solar rotation they come into "geoeffective position" such that the solar wind originating from them can hit the Earth, so they are sources of "recurrent" (regularly reoccurring every 27 days) geomagnetic activity. Coronal holes are open magnetic field regions related to the solar poloidal magnetic field and have a clear solar cycle dependence. The high speed solar wind streams are most numerous and most intense near sunspot minimum when the open flux originates mainly from the large polar coronal holes, whereas at sunspot maximum it is rooted in small, lower-latitude holes (Wang et al., 2000). The outflow speeds for the equatorial coronal holes are 3-4 times lower than those in polar coronal holes (Miralles et al., 2004).

IDENTIFICATION OF THE SOLAR WIND DRIVERS

The period which we have chosen for our study is 1995-2006 because in this time several satellines have been providing continuous data. It covers a complete solar cycle, from sunspot minimum to sunspot minimum.

In order to study the effects of different solar drivers on the atmosphere and geomagnetic disturbances, we first have to compile lists of these drivers. In general, this is not a straightforward procedure because, apart from the solar flares, different authors apply different criteria to identify solar drivers.

Solar flares

To study the effects of solar flares, we use the list of X-class solar flares obtained from the server of the NOAA Space Environment Center http://www.sec.noaa.gov/ftpdir/indices/old_indices/. The X-class solar flares are the most powerful flares according to their X-ray brightness in the wavelength range 1 to 8 Angstroms, with peak intensity $I \geq 10^{-4}$ W/m^2. As solar flares can be accompanied by coronal mass ejections, all cases when a solar flare was followed within 2-5 days by a coronal mass ejection or a magnetic cloud, were removed from both lists. Table 1 gives the remaining major solar flares used in this study.

Table 1. Major solar flares

Year month day	2000 6 7	2003 3 18
1996 7 9	2000 6 18	2003 6 9
1997 11 4	2000 7 14	2003 6 15
1997 11 6	2000 11 24	2004 2 26
1997 11 27	2001 4 3	2004 7 15
1998 4 23	2001 4 6	2004 7 16
1998 4 27	2001 4 12	2004 8 13
1998 5 2	2001 6 23	2004 8 18
1998 5 6	2001 8 25	2004 10 30
1998 8 19	2001 9 24	2004 11 10
1998 8 24	2001 10 22	2005 1 1
1998 11 22	2001 10 25	2005 1 15
1998 11 23	2001 11 25	2005 1 20
1998 11 24	2001 11 11	2005 7 30
1998 11 28	2001 11 13	2005 9 7
1999 8 2	2001 12 28	2005 9 8
1999 8 28	2002 7 3	2005 9 9
1999 10 14	2002 7 15	2005 9 10
1999 11 27	2002 7 18	2005 9 13
2000 2 5	2002 7 20	2005 9 15
2000 3 2	2002 7 23	2006 12 5
2000 3 22	2002 8 3	2006 12 6
2000 3 24	2002 8 21	2006 12 13
2000 6 6	2002 10 31	2006 12 14

Magnetic clouds

As magnetic clouds are a subclass of coronal mass ejections, in order to identify magnetic clouds first the CME's have to be identified. There is a disagreement in the literature about the criteria to identify CME's, and the lists of CME's compiled by different authors do not include the same events. The most popular criteria for CME's are: bidirectional strahl electrons (Gosling et al., 1987) indicating that both ends of the magnetic field tube are attached to the Sun; enhanced alpha/proton ratio (Borrini et al., 1982); decreasing velocity (Klein and Burlaga, 1982), low proton (Richardson and Cane, 1995) or electron (Montgomery et al., 1974) temperature, low density (Richardson et al., 2000), all indicating expanding structures; unusual elemental (Schwenn et al., 1980) or charge (Ipavich et al., 1986) solar wind composition, etc.

Of these, not all features are present in all CME's, and not all data are easily available for the whole period studied. Therefore, as a first step for the detection of CME's we applied the criterion of Richardson and Cane (1995) for abnormally low proton temperature.

By "abnormally low temperature" they denoted proton temperature $T_p < 0.5T_{ex}$, where T_{ex} is the proton temperature "expected" from the empirically determined correlation between the temperature and solar wind velocity V_{sw} (Lopez and Freeman, 1986):

$T_{ex} = (0.0106V_{sw} - 0.287)^3/R$ if $V_{sw} < 500$ km/s
$T_{ex} = (0.77V_{sw} - 265)/R$ if $V_{sw} \geq 500$ km/s

The criterion for $T_p < 0.5T_{ex}$ for at least 5 hours was tested against the lists of CME's in 1997 (a year with a high number of CME's and a low number of high speed solar wind streams) identified by different authors. It was found that this criterion detects all CME's, but identifies as CME's about 3 times more events which are not CME's.

As we are actually interested not just in CME's in general but in magnetic clouds, we added the requirement for high magnetic field magnitude ($B \geq 10$ nT) and low plasma beta (the ratio of plasma pressure to magnetic pressure), beta ≤ 0.8 for at least 5 hours. We then completed the resulting list with the additional events in the lists of magnetic clouds given by Fenrich and Luhmann (1998), Leamon and Canfield (2002), Vilmer et al. (2003), (Gopalswamy, 2006), SOHO LASCO CME catalog (http://cdaw.gsfc.nasa.gov/CME_list/), WIND MFI magnetic cloud list (http://sprg.ssl.berkeley.edu/~davin/clouds/cloud_list.html). Finally, all the events in this extended list were subjected to visual inspection, and all events without a clear magnetic field rotation were removed. This leaves us with 198 magnetic cloud events given in Table 2 together with their direction of rotation (R=right-handed, L=left-handed).

Table 2. Magnetic clouds

Year month day helicity	1995 3 4 L	1995 7 23 R
1995 1 8 R	1995 3 23 L	1995 8 22 R
1995 2 8 L	1995 4 3 L	1995 10 10 R
1995 2 9 L	1995 6 30 L	1995 10 18 R

1995 12 16 L
1996 2 15 L
1996 4 26 L
1996 5 27 L
1996 7 1 L
1996 10 23 R
1996 8 7 R
1996 12 24 R
1997 1 10 R
1997 2 5 L
1997 2 10 L
1997 4 11 R
1997 4 21 R
1997 5 15 L
1997 5 20 R
1997 5 26 R
1997 6 7 R
1997 6 9 R
1997 6 19 R
1997 7 15 L
1997 8 3 L
1997 9 3 R
1997 9 18 R
1997 9 22 L
1997 10 1 L
1997 10 10 R
1997 10 27 L
1997 11 4 L
1997 11 7 R
1997 11 22 R
1997 12 10 L
1998 1 7 L
1998 1 8 L
1998 1 22 L
1998 1 28 L
1998 1 30 R
1998 2 4 L
1998 2 18 R
1998 3 4 L
1998 4 2 L
1998 6 2 L
1998 6 6 L
1998 6 14 R
1998 6 24 L
1998 7 12 L
1998 8 6 L
1998 8 7 L
1998 8 20 R
1998 9 25 L
1998 10 19 L
1998 11 8 L
1998 11 9 R
1998 11 14 R
1998 12 11 R
1998 12 26 R
1999 2 18 L
1999 2 19 L
1999 4 16 L
1999 4 21 L
1999 5 18 L
1999 5 28 L
1999 7 6 R
1999 7 8 L
1999 8 9 L
1999 8 22 R
1999 9 15 L
1999 9 22 L
1999 10 21 R
1999 11 14 L
2000 1 7 L
2000 2 12 R
2000 2 21 L
2000 2 21 R
2000 3 30 R
2000 4 4 L
2000 4 7 R
2000 5 7 L
2000 6 6 L
2000 6 24 L
2000 7 7 L
2000 7 15 L
2000 7 28 L
2000 8 12 L
2000 9 4 L
2000 9 6 R
2000 9 18 L
2000 10 3 R
2000 10 5 R
2000 10 6 L
2000 10 11 L
2000 10 13 R
2000 10 28 L
2000 11 6 L
2000 11 29 L
2000 12 4 R
2000 12 29 L
2001 1 30 L
2001 3 4 R
2001 3 20 L
2001 3 31 L
2001 4 4 L
2001 4 12 R
2001 4 18 L
2001 4 22 L
2001 4 29 L
2001 5 28 L
2001 7 10 R
2001 8 18 R
2001 9 30 L
2001 10 3 L
2001 10 21 R
2001 11 1 L
2001 11 6 R
2001 11 15 R
2001 11 24 L
2001 12 28 L
2002 3 19 R
2002 3 24 R
2002 4 18 R
2002 4 20 L
2002 4 23 R
2002 5 10 R
2002 5 19 R
2002 5 23 L
2002 7 29 R
2002 8 1 R
2002 8 2 L
2002 8 20 L
2002 8 26 R
2002 9 3 R
2002 9 7 L
2002 9 30 L
2002 10 2 R
2002 10 14 R
2002 11 27 L
2003 2 1 L
2003 2 18 L
2003 3 20 R

2003 5 9 L	2004 1 22 L	2005 6 15 L
2003 5 30 R	2004 2 11 R	2005 6 23 R
2003 6 14 L	2004 4 4 L	2005 7 10 L
2003 6 17 L	2004 4 9 R	2005 7 17 R
2003 7 6 R	2004 4 12 R	2005 8 13 L
2003 7 10 R	2004 4 30 R	2005 8 24 R
2003 7 23 R	2004 7 22 R	2005 8 31 R
2003 8 5 L	2004 7 24 R	2005 10 7 L
2003 8 18 R	2004 7 27 R	2005 10 31 R
2003 10 22 L	2004 8 29 R	2005 12 24 L
2003 10 24 L	2004 9 17 L	2005 12 31 R
2003 10 25 R	2004 11 7 L	2006 2 5 R
2003 10 26 L	2004 11 10 L	2006 4 13 L
2003 10 29 L	2005 1 21 L	2006 5 4 L
2003 10 31 R	2005 5 15 L	2006 9 30 L
2003 11 7 L	2005 5 20 L	2006 11 29 R
2003 11 20 R	2005 5 29 L	2007 1 14 L
2004 1 9 L	2005 6 12 L	2007 3 24 R

High speed solar wind

For high speed solar wind there are also different definitions, and respectively, different lists of events. The required characteristics are usually a peak velocity of over 450 (Intriligator, 1975), 500 (Broussard et al., 1978; ISTP catalog (http://pwg.gsfc.nasa.gov/scripts/sw-cat/Catalog_categories.html)) or 650 km/s (Feldman et al., 1976), increasing velocity without a specified increase (Jian et al., 2006) or with a required increase of at least 80 (Lindblad and Lundstedt, 1981), 100 (Maris and Maris, 2002) or 150 km/s (Gosling et al., 1976), high proton temperature and low plasma density (ISTP catalog), maximum in the perpendicular pressure (Jian et al., 2006).

Our criteria include an increase of the solar wind velocity by at least 100 km/s in no more than one day to at least 500 km/s for at least 5 hours, accompanied by high temperature and low density. In this way fast coronal mass ejections are eliminated which may also have high speed and a sharp speed increase, but have low temperature. The list of our high speed solar wind events is given in Table 3.

Table 3. High speed solar wind streams

Year month day	1995 4 7	1995 8 13
1995 1 2	1995 4 26	1995 9 5
1995 1 18	1995 5 2	1995 9 10
1995 1 22	1995 5 23	1995 9 12
1995 1 28	1995 5 30	1995 10 4
1995 2 11	1995 6 19	1995 10 7
1995 2 28	1995 6 25	1995 10 20
1995 3 10	1995 7 16	1995 11 1
1995 3 26	1995 8 7	1995 11 5

1995 11 27
1995 12 24
1996 1 2
1996 1 14
1996 1 29
1996 2 11
1996 2 26
1996 3 11
1996 3 21
1996 4 14
1996 4 17
1996 7 3
1996 7 31
1996 8 14
1996 8 16
1996 8 29
1996 9 10
1996 9 19
1996 9 26
1996 10 1
1996 10 8
1996 10 17
1996 10 28
1996 11 17
1996 11 24
1996 12 10
1996 12 15
1997 1 26
1997 1 28
1997 2 8
1997 2 17
1997 2 20
1997 2 28
1997 3 11
1997 3 26
1997 3 30
1997 4 16
1997 5 1
1997 6 27
1997 8 13
1997 8 28
1997 9 3
1997 9 27
1997 10 25
1997 11 30
1998 2 11
1998 3 10
1998 3 21
1998 4 17
1998 5 8
1998 5 16
1998 6 3
1998 7 16
1998 7 23
1998 8 23
1998 10 7
1998 10 20
1998 10 27
1998 11 23
1998 12 16
1999 1 6
1999 2 11
1999 2 14
1999 3 1
1999 3 4
1999 3 14
1999 3 29
1999 4 4
1999 4 10
1999 4 27
1999 4 29
1999 5 18
1999 5 23
1999 5 25
1999 6 8
1999 6 27
1999 7 22
1999 7 30
1999 8 6
1999 8 15
1999 9 7
1999 9 12
1999 9 26
1999 10 5
1999 10 10
1999 10 15
1999 10 22
1999 11 7
1999 11 16
1999 12 3
1999 12 24
1999 12 30
2000 1 10
2000 1 27
2000 2 5
2000 2 23
2000 3 12
2000 3 22
2000 3 24
2000 4 16
2000 4 19
2000 5 22
2000 5 29
2000 6 15
2000 7 3
2000 8 5
2000 8 14
2000 8 28
2000 9 24
2000 9 25
2000 10 15
2000 10 22
2000 11 4
2000 11 24
2000 12 8
2001 2 6
2001 2 13
2001 2 26
2001 2 28
2001 5 8
2001 5 23
2001 6 1
2001 6 9
2001 6 19
2001 7 16
2001 7 24
2001 7 31
2001 8 10
2001 8 21
2001 9 3
2001 9 15
2001 10 11
2001 12 3
2001 12 15
2001 12 24
2002 1 19
2002 2 5
2002 2 11

2002 3 3
2002 3 26
2002 3 30
2002 4 27
2002 5 12
2002 5 27
2002 6 18
2002 7 5
2002 7 12
2002 8 14
2002 9 11
2002 9 16
2002 10 7
2002 10 18
2002 10 24
2002 11 10
2002 11 20
2002 12 6
2002 12 13
2002 12 19
2002 12 22
2002 12 26
2003 1 2
2003 1 10
2003 1 19
2003 1 22
2003 2 4
2003 2 14
2003 2 26
2003 3 3
2003 3 14
2003 3 30
2003 4 9
2003 4 14
2003 5 27
2003 6 19
2003 6 27
2003 7 3
2003 7 19
2003 7 26
2003 8 7
2003 8 11
2003 8 21
2003 8 29
2003 9 4
2003 9 8
2003 9 16
2003 9 26
2003 10 1
2003 10 6
2003 10 14
2003 11 10
2003 11 29
2003 12 7
2003 12 20
2003 12 27
2004 1 4
2004 1 15
2004 1 30
2004 1 31
2004 1 2
2004 2 5
2004 2 12
2004 2 28
2004 3 9
2004 3 27
2004 4 6
2004 4 21
2004 4 25
2004 4 28
2004 5 5
2004 5 20
2004 6 28
2004 7 11
2004 7 17
2004 7 19
2004 8 7
2004 8 9
2004 8 25
2004 8 31
2004 9 5
2004 9 22
2004 10 13
2004 10 29
2004 11 19
2004 11 25
2004 11 29
2004 12 16
2004 12 25
2005 1 1
2005 1 12
2005 2 7
2005 2 24
2005 3 6
2005 3 24
2005 4 4
2005 4 11
2005 4 19
2005 4 30
2005 5 8
2005 6 4
2005 6 16
2005 7 1
2005 7 13
2005 7 20
2005 7 28
2005 8 1
2005 8 6
2005 8 15
2005 9 2
2005 10 25
2005 11 2
2005 11 30
2005 12 11
2005 12 19
2005 12 27
2006 1 23
2005 1 26
2006 2 15
2006 2 20
2006 3 10
2006 3 18
2006 4 10
2006 4 21
2006 5 6
2006 5 11
2006 5 18
2006 6 1
2006 6 6
2006 6 14
2006 6 27
2006 7 4
2006 7 11
2006 7 28
2006 7 31
2006 8 7
2006 8 27
2006 9 4

2006 9 17	2006 11 9	2007 2 27
2006 9 24	2006 11 16	2007 3 6
2006 10 1	2006 12 18	2007 3 12
2006 10 7	2007 1 1	2007 3 27
2006 10 13	2007 1 11	2007 4 1
2006 10 20	2007 1 29	
2006 10 28	2007 2 12	

GEOMAGNETIC DISTURBANCES

Geomagnetic disturbances are quantified by two main indices: Kp and Dst. Kp index (Bartels et al., 1939) is obtained from a number of magnetometer stations at mid-latitudes. It is mainly sensitive to the position and intensity of the auroral zone. Dst index (Sugiura, 1964) is obtained from magnetometer stations near the equator and is sensitive to the intensity of the magnetospheric ring current. In the present study we compare the changes in both indices in response to solar flares, high speed plasma wind and magnetic clouds.

Kp index

Fig.1. presents the reaction of the Kp index to the three types of solar drivers. It can be seen that solar flares not accompanied by coronal mass ejections have little effect on Kp index. Magnetic clouds and high speed solar wind cause comparable disturbances, a little stronger for magnetic clouds, and with the characteristic "calm before the storm" – the decrease a couple of days before the maximum disturbance – in the case of high speed streams (Borovsky and Steinberg, 2006).

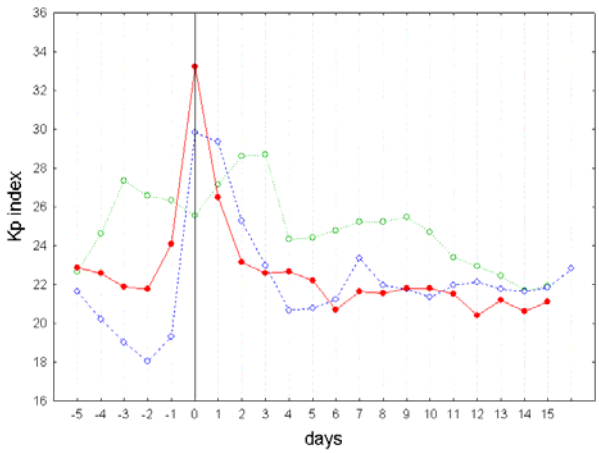

Fig.1. Superposed epochs analysis of Kp index relative to the days with solar flares (dotted line, green), high speed solar wind streams (dashed line, blue) and magnetic clouds (solid line, red).

Another difference which can be noticed in Fig.1 is that the high levels of geomagnetic disturbances caused by high speed solar wind persist longer than in the case of magnetic clouds as noticed by Borovsky and Denton (2006). What we additionally note is that the time for recovery to the pre-storm levels depends on the solar cycle phase: 2 days in sunspot minimum versus 4 days in sunspot maximum for magnetic clouds, and 2 days in sunspot maximum versus 4 days on sunspot declining and minimum phase for high speed wind.

In the case of high speed solar wind, the disturbance depends on the background state of the atmosphere – the phase of the quasibiennial oscillation of equatorial stratospheric winds (QBO). In QBO Westerly, the disturbance is bigger and lasts longer than in QHO Easterly (Fig.2).

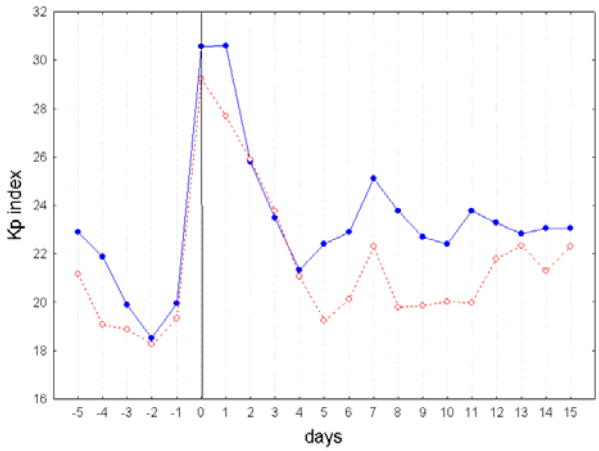

Fig.2. Kp index for high-speed solar wind in Westerly (solid line, blue) and Easterly (dashed line, red) phases of QBO.

The geoeffectiveness of magnetic clouds as measured by Kp index is more sensitive to the handedness of the cloud than to the phase of QBO: right-handed clouds lead to higher Kp-index (Fig.3).

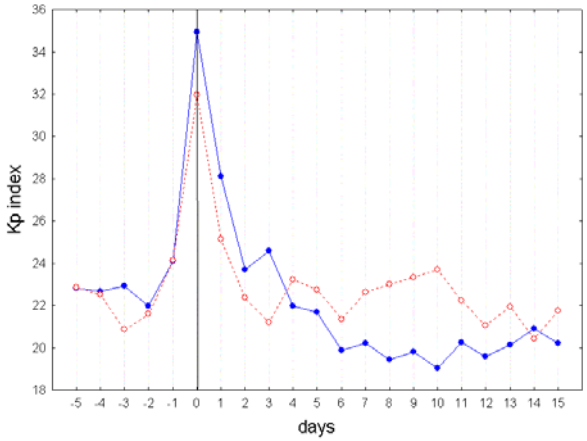

Fig.3. Kp-index for magnetic clouds with right-handed rotation (solid line, blue) and left-handed rotation (dashed line, red).

Dst index

As in the case of Kp index, solar flares not followed by mass ejections practically don't cause geomagnetic disturbances as measured by the Dst index. Comparing high speed solar wind and magnetic clouds, the magnetic clouds lead to much stronger (Dst more negative) and longer lasting geomagnetic activity (Fig.4). That is, hogh speed solar wind leads to longer lasting storms (Borovsky and Denton, 2006) only as measured by Kp index but not by Dst index. The ring current activity to which Dst index is more sensitive, lasts longer in the case of magnetic clouds.

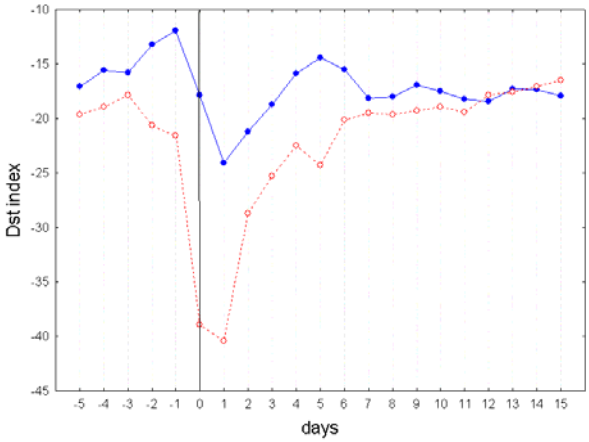

Fig.4. Superposed epochs analysis of Dst index relative to the days with high speed solar wind streams (solid line, blue) and magnetic clouds (dashed line, red).

Again, high speed solar wind leads to stronger and longer lasting disturbances in the Westerly phase of QBO (Fig.5). In Figs. 4 and 5 it is clearly seen that the maximum disturbance caused by high speed solar wind is on the day following the stream, as compared to the disturbance on the day of the high speed solar wind measured by Kp index (Figs. 1 and 2). This is due to the longer time needed for the ring current to build up than for the auroral zone to react to the driver.

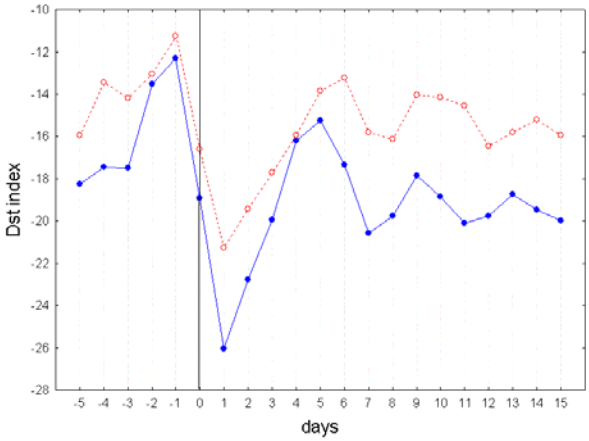

Fig.5. Dst index for high-speed solar wind in Westerly (solid line, blue) and Easterly (dashed line, red) phases of QBO.

Geomagnetic disturbances caused by magnetic clouds as measured by Dst index have no difference in QBO Westerly and Easterly phase, but there is a difference between right-handed and left0handed clouds. The recovery time is the same but the maximum disturbance is bigger for left-handed clouds (Fig.6). In both cases the disturbance begins on the day of the event and deepens still more on the following day. This is related to the different parts of the magnetic cloud which can cause geomagnetic storms (the compressed shock preceding the cloud, the cloud itself, and the trailing end).

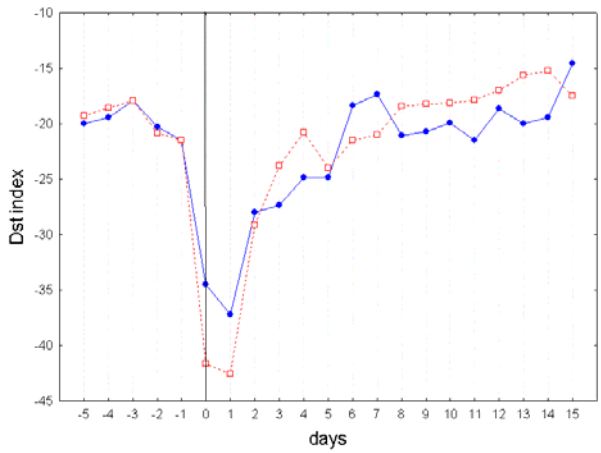

Fig.6. Dst-index for magnetic clouds with right-handed rotation (solid line, blue) and left-handed rotation (dashed line, red).

ATMOSPHERIC CIRCULATION

Atmospheric circulation is the system of atmospheric motions over the Earth on the scale of the whole globe (general atmospheric circulation), or over a certain region with its specific features (local circulation). There are two basic types of atmospheric circulation: zonal and meridional. Zonal circulation is characterized by westerly (from the west) winds at midlatitudes, and low amplitude waves in the troposphere moving quickly from west to east. When a meridional circulation prevails, the meridional transfer is intensified and stationary high amplitude waves are observed.

LOW ATMOSPHERE

As a measure for the zonality of the atmospheric circulation, we use the index of the North Atlantic Oscillation (NAO). The North Atlantic Oscillation is a north-south see-saw oscillation between the atmospheric centers of action in the Atlantic: the Icelandic Low at high-latitude, and Azores High in the subtropics (the centers of action are isolated regions of persistent high or low pressure). NAO index is defined as the difference between the normalized sea-level pressure in these two centers of action. When the high pressure in the Azores High is even higher than average, usually the low pressure in the Icelandic Low is even lower than average, and NAO is in positive phase characterized by enhanced midlatitude westerly winds across the Atlantic onto Europe – that is, enhanced zonality of the circulation. In the reverse case, when the two centers of action are weakened (lower than average high pressure in the Azores High and higher than average

low pressure in the Icelandic Low), NAO is negative and zonal circulation is weakened while meridional circulation is enhanced.

To study the relation between century-scale vatiations in solar activity and atmospheric circulation, we use a reconstruction of NAO with monthly values since 1659 and seasonal values since 1500 (Luterbacher et al., 1999, 2001). Of them, we study the period since 1611 for which the group sunspot number is available as a measure of the yearly level of solar activity (Hoyt and Schatten, 1998). NAO index is calculated as the average of the three winter months, December, January and February. In Fig.7, NAO index is presented (solid line) together with the group sunspot number Rg (dotted line) and the International sunspot number available since 1700 (dashed line).

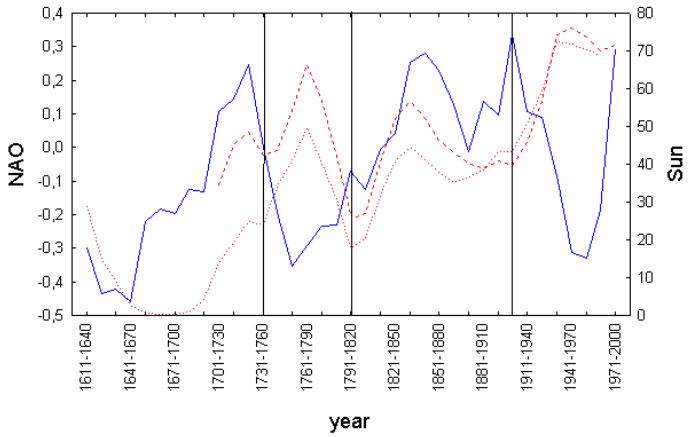

Fig.7. Solid blue line: NAO index (Luterbacher et al., 2001); red dashed line: International sunspot number; red dotted line: Group sunspot number (Hoyt and Schatten, 1998). 30-year averages.

The vertical lines divide the period into epochs with positive and negative correlations between the long-term variations of NAO and solar activity. In the 20th century the correlation is negative, but in the 19th century it is positive, negative again in the 18th century, and positive again in the 17th century. The correlation in the last period is not statistically significant, but it should be noted that this is the period of the Maunder minimum when sunspot activity was atypical. The change in the correlation between the long-term variations of NAO and solar activity coincides with the change in the correlation between surface air temperature and solar activity in the 11-year sunspot cycle, which is supposed to coincide with the changes in the long-term solar activity asymmetry (Georgieva and Kirov, 2000). We can therefore speculate that when the southern solar hemisphere is more active, increasing solar activity in the secular solar cycle leads to strengthening of the zonal atmospheric circulation, and when the northern solar hemisphere is more active, increasing solar activity in the secular solar cycle leads to weakening of the zonal circulation.

To study the short-term reaction of the circulation to different solar drivers, we calculate the daily differences in the atmospheric pressure between the Azores High and Icelandic Low. The data are from the project EMULATE (European and North Atlantic daily to

MULtidecadal climATE variability) which provides the daily gridded sea level pressure data over the extratropical Atlantic and Europe (70°-25° N by 70° W-50° E, 5^{o}x5^{o} boxes, available online at http://www.cru.uea.ac.uk/cru/ projects/emulate/). From this data set we use the boxes containing the Azores High (31.6^{o}N, 32.7^{o}W) and the Icelandic Low (59.6^{o} N, 33.1^{o} W), and calculate their difference as a measure of the NAO index.

Solar flares

Fig.8, a and b, present the pressure in these two centers of action, and their difference as a measure of the NAO index, respectively, relative to the days with X-class solar flares.

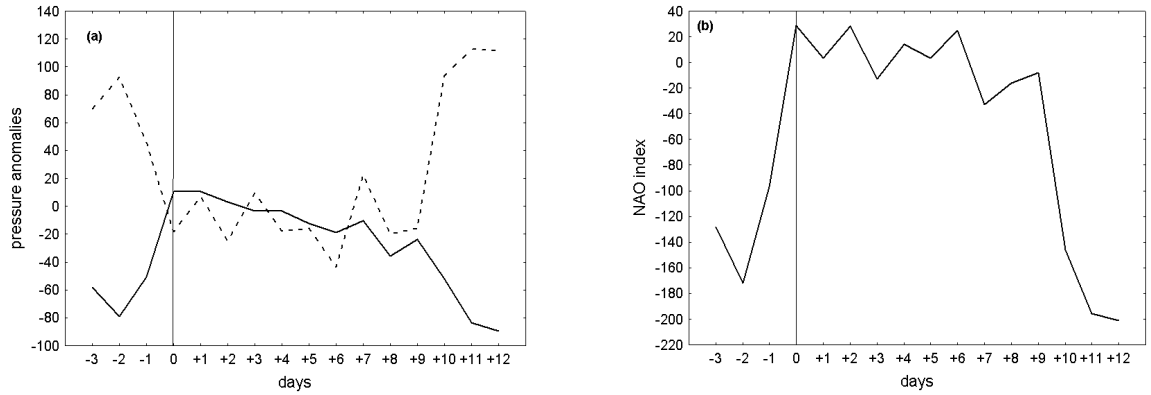

Fig.8. (a): surface pressure anomalies in the Azores High (solid line) and Icelandic Low (dashed line) relative to days with X-class solar flares; (b): NAO index relative to days with X-class solar flares.

High speed solar wind

The effect of high speed solar wind is an increased pressure impulse with a duration of about 5 days, propagating from high to low latitudes (Fig.9a). This high pressure wave reaches the Azores with a reduced magnitude with a delay of three days, when the pressure in Iceland has already decreased. The net result is an increase in the pressure difference between low and high latitudes and hence in the zonal circulation with a maximum 4 days after the high speed solar wind hits the Earth (Fig.9b).

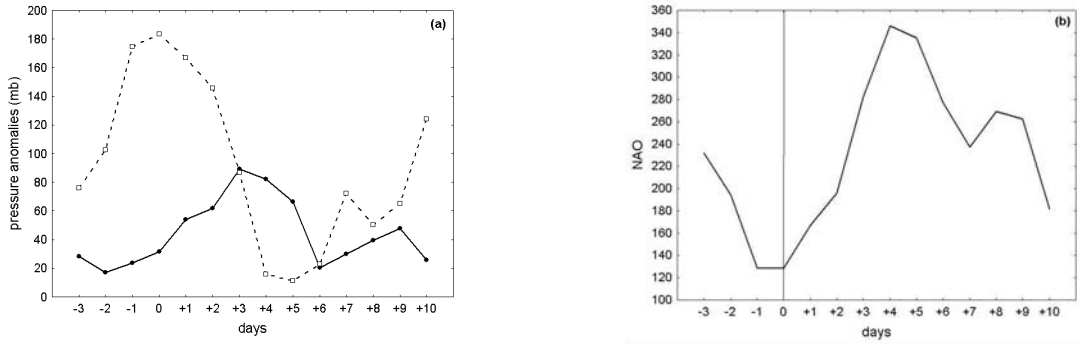

Fig,9. (a) Pressure anomalies in the Azores High (solid line) and Icelandic Low (dashed line) relative to days with high speed solar wind streams; (b) pressure difference between the Azores and Iceland.

Magnetic clouds

Fig.10 presents the reaction of the sea level pressure in the Azores and Iceland, and of their difference as a proxy for zonal atmospheric circulation, for cases of encounter of interplanetary magnetic clouds.

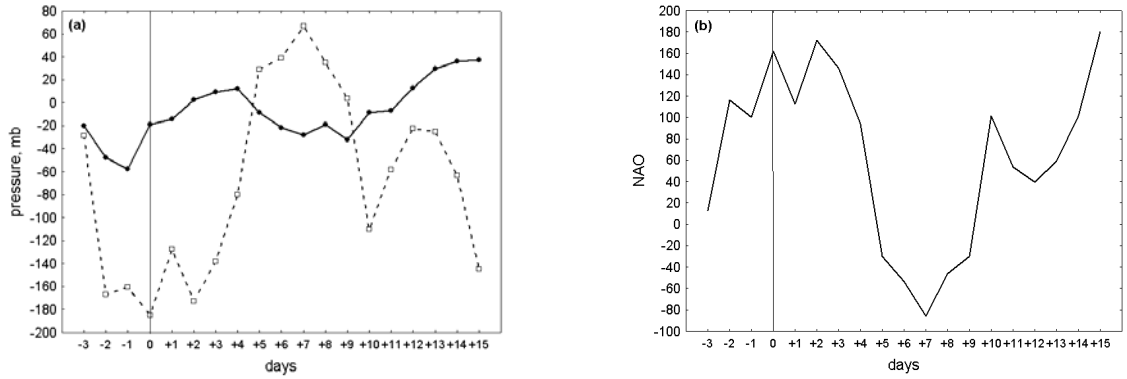

Fig.10. (a): Pressure anomalies in the Azores (solid line) and Iceland (dashed line) relative to days of encounter of magnetic clouds; (b): NAO index as the difference in the pressure between Azores and Iceland relative to the days of encounter of magnetic clouds.

The main reaction is observed at high latitudes, as should be expected taking into account that the effect of magnetic clouds is strongest at high latitudes. The pressure at low latitudes practically doesn't react to magnetic clouds. Consequently, the changes in NAO index are determined by the high latitude processes. NAO has a prolonged deep minimum starting two days after the magnetic cloud encounter, and reaching its lowest values five days later. A more careful inspection reveals that on the day of the encounter of a magnetic cloud and shortly prior to it NAO index has a maximum, and the pressure in Iceland has a minimum. This maximum in NAO and the minimum in Iceland pressure vanish if we exclude the fast magnetic clouds with preceding shocks. Obviously, the shock itself, irrespective of its causes, always leads to a decrease in the pressure at high latitudes. It should be noted here that according to the criteria which we have adopted, the beginning of the magnetic cloud is considered the beginning of the magnetic field rotation, while normally the shock precedes it by a few hours to a day or two.

TROPOSPHERE

To study the effects of the different solar drivers throughout the troposphere, we use the indices of the Northern Annular Mode (NAM) and Southern Annular Mode (SAM). The Northern Annular Mode is the hemispheric-scale analog of NAO. This is the dominant pattern of non-seasonal sea-level pressure variations north of 20^{o}N, and it is characterized by sea-level pressure anomalies of one sign in the Arctic and anomalies of the opposite sign centered about 37-45^{o}N. In the high phase of the index, the pressure is below normal in the Arctic and the surface westerlies in the north Atlantic are enhanced (Baldwin, 2001). SAM index is the southern analog of NAM index, and is expressed as the difference between the pressure anomalies over the Antarctic and at southern

midlatitudes. The daily values of NAM and SAM at 17 pressure levels from 1000 hPa (surface) to 10 hPa (~32 km) are available online at http://www.nwra.com/resumes/baldwin/nam.php. For our investigation of the solar drivers effects in the troposphere, we use data for the pressure levels from 1000 to 200 hPa (the upper boundary of the troposphere).

Solar flares

Fig.11 a and b present the changes in NAM and SAM index at tropospheric heights, respectively, after powerful (X-class) solar flares.

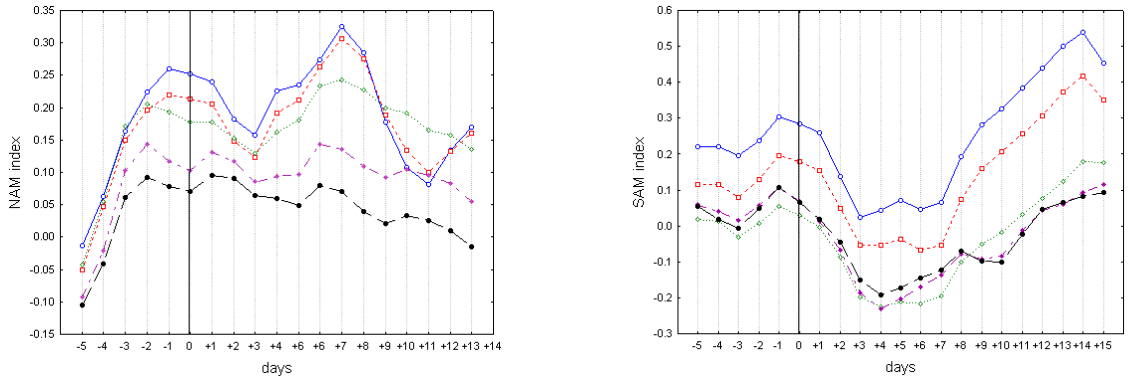

Fig.11. Reaction of the NAM index (left) and SAM index (right) to X-class solar flares: solid blue line – 1000 hPa; red dashed line – 850 hPa, green dotted line – 500 hPa; violet dash-dotted line – 250 hPa; black long-dashed line – 200 hPa.

In Fig. 12 and 13 are presented the cases separately for QBO Westerly and Easterly, respectively.

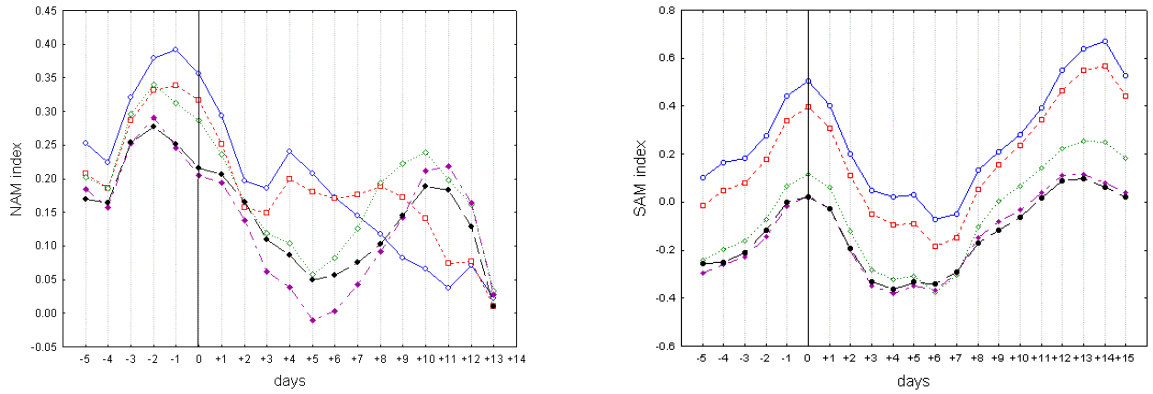

Fig.12. Reaction of the NAM index (left) and SAM index (right) to X-class solar flares for cases of QBO Westerly; the legend is like in Fig.11.

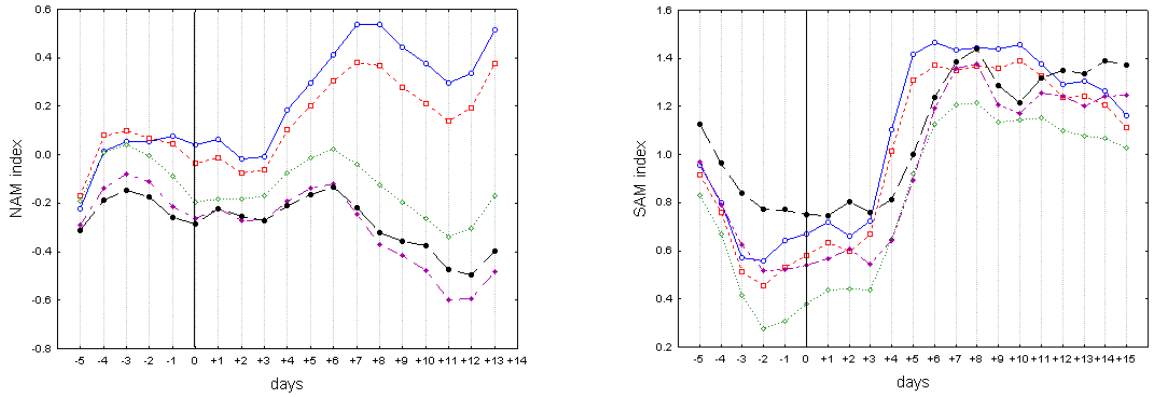

Fig.13. Reaction of the NAM index (left) and SAM index (right) to X-class solar flares for cases of QBO Easterly; the legend is like in Fig.11.

In all three figures, some similarity can be seen between the hemispheres. Fig.11 with all events included is in fact a superposition of two different cases: for QBO Westerly when solar flares lead to a decrease in NAM and SAM indices about 4-5 days after the flare, and for QBO Easterly when the reaction is an increase in both indices 7-8 days after the flare. The difference between the two hemispheres is that while in the south the values at all levels change synchronously, in the north the reaction in QBO Easterly is mainly seen close to the surface (1000 and 850 hPa), and in QBO Westerly, on the contrary, the reactсдn is confined in the lower atmosphere.

High speed solar wind

The reaction of NAM and SAM indices to high speed solar wind streams are demonstrated in Fig.14 (all cases), Fig. 15 (QBO Westerly) and Fig.16 (QBO Easterly).

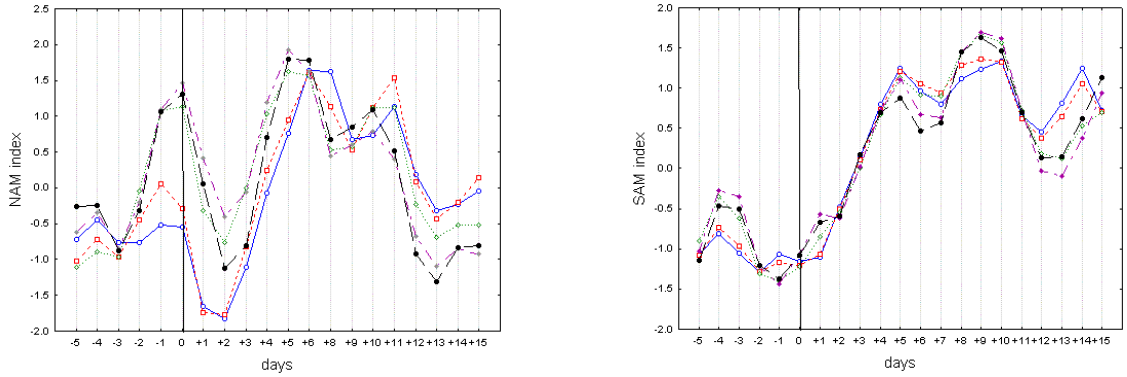

Fig.14. Reaction of the NAM index (left) and SAM index (right) to high speed solar wind streams; the legend is like in Fig.11.

In both hemispheres, the main effect is the increase in the zonality index 6-10 days after the event. The differences are that in the north there is an increase also on the day of the event, especially at higher levels, and in the south it takes longer for the index to get back to its undisturbed level.

The reaction of the two hemispheres is identical in the case of QBO Westerly: a decrease on the day following the event, more expressed in the south and a strong increase 5-8 days later (Fig. 15).

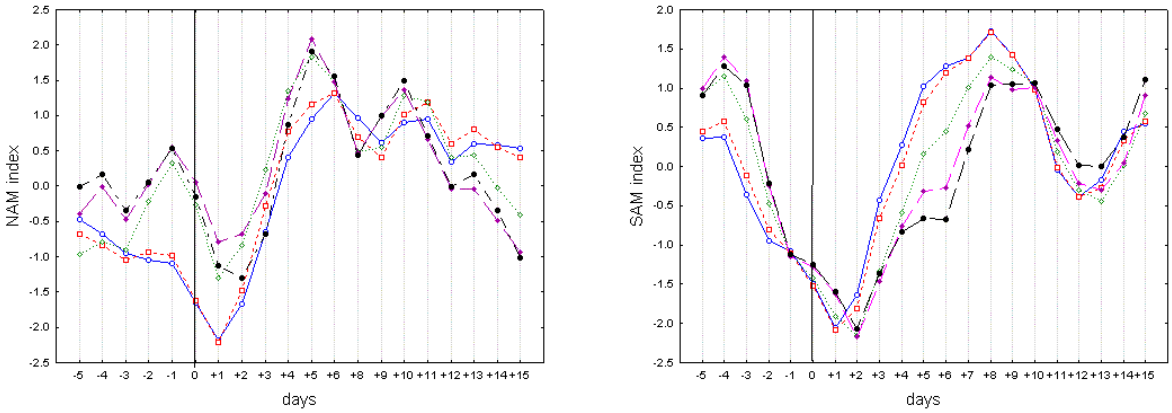

Fig.15. Reaction of the NAM index (left) and SAM index (right) to high speed solar wind streams in cases of QBO Westerly; the legend is like in Fig.11.

However, in QBO Easterly the effects are quite opposite in the north and in the south: a persistent decrease in the zonality in the north versus a persistent increase in the south (Fig.15).

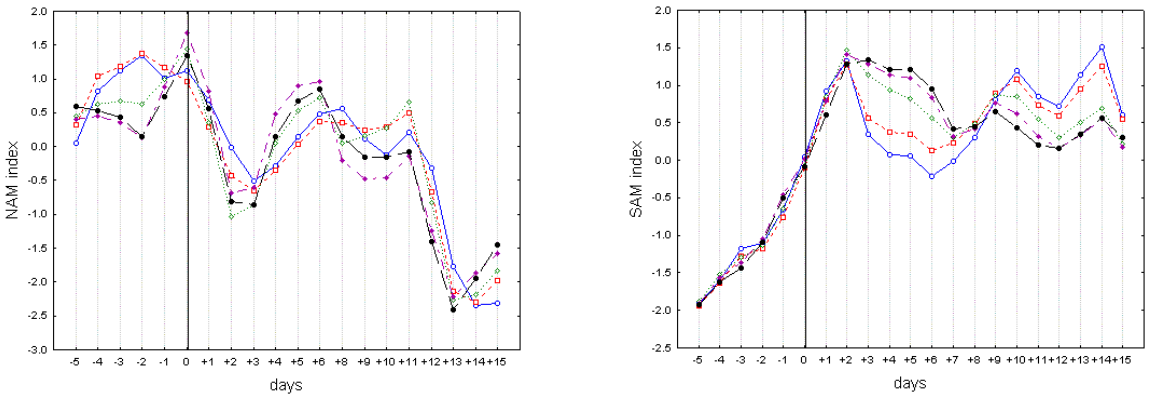

Fig.15. Reaction of the NAM index (left) and SAM index (right) to high speed solar wind streams in cases of QBO Easterly; the legend is like in Fig.11.

Magnetic clouds

Fig.16 presents NAM and SAM index relative to zhe days with magnetic clouds. The reaction in the two hemispheres is quite different. While in the north the effect is a decrease in the zonality index about 5 days after the event, more pronounced at lower levels while at higher levels there is a high long-term increase, in the south magnetic clouds cause a persistent decrease at all levels. In Fig.17 and 18 it is seen that in the northern hemisphere this is a superposition of the decrease at all levels in QBO Westerly and the increase at higher levels in QBO Easterly, while in the southern hemisphere there

is a general decrease in QBO Westerly and a well pronounced peak in the zonal flow after magnetic clouds in QBO Easterly.

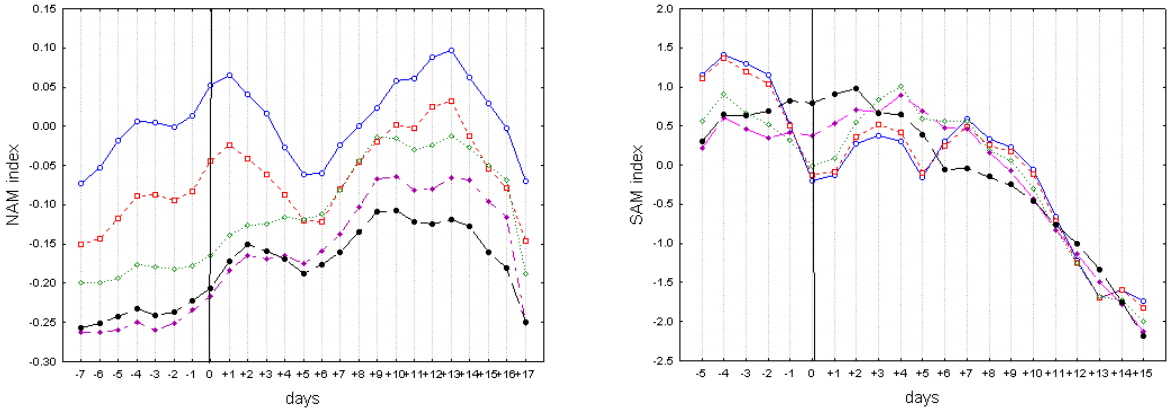

Fig.16. Reaction of the NAM index (left) and SAM index (right) to magnetic clouds; the legend is like in Fig.11.

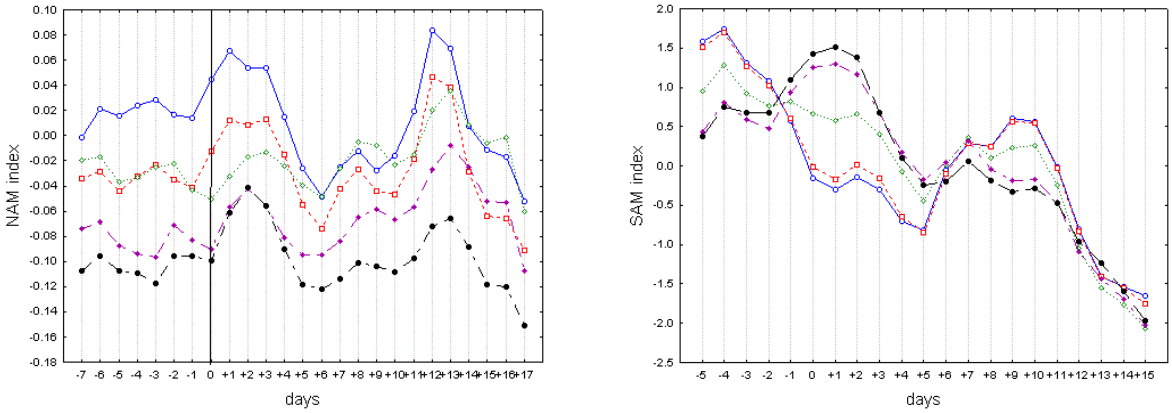

Fig.17. Reaction of the NAM index (left) and SAM index (right) to magnetic clouds in QBO Westerly; the legend is like in Fig.11.

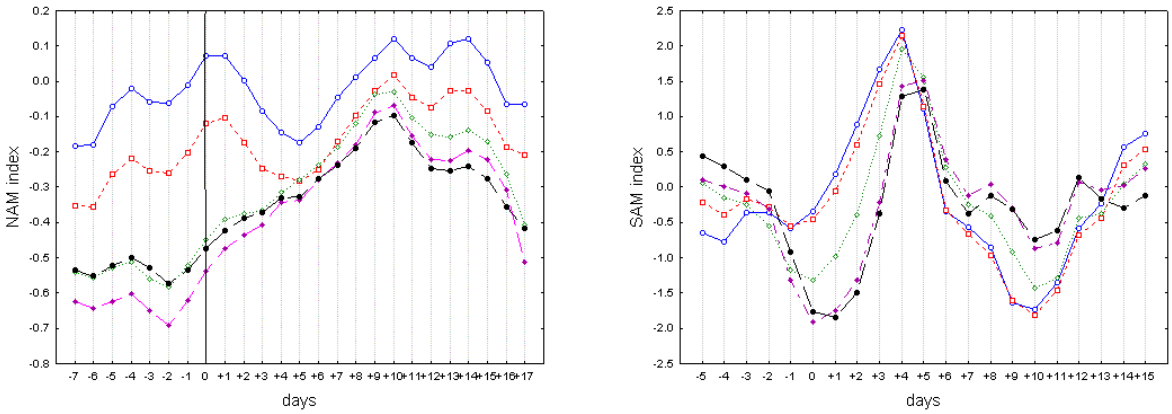

Fig.18. Reaction of the NAM index (left) and SAM index (right) to magnetic clouds in QBO Easterly; the legend is like in Fig.11.

The reaction in the south is not much different for left-handed and right-handed clouds, while in the north the zonality index increases after left-handed clouds and decreases after right-handed clouds (Fig.19).

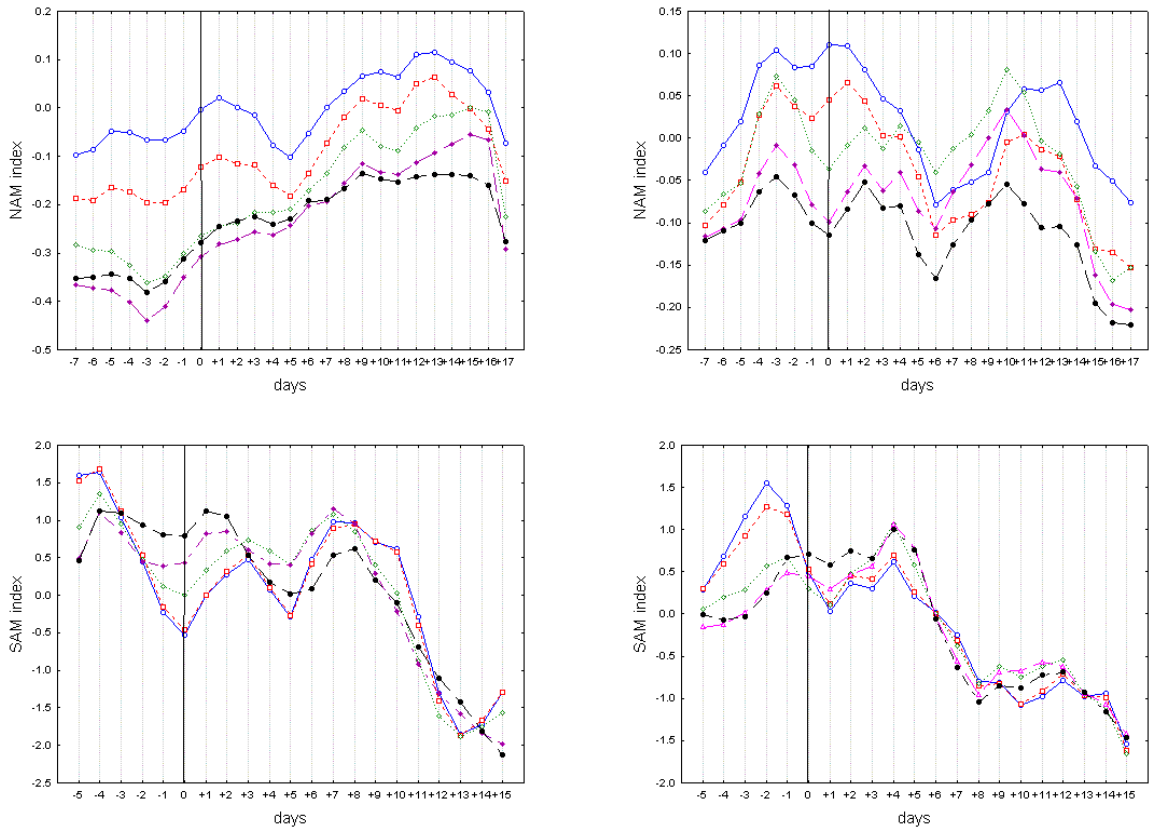

Fig.19. Reaction of the NAM index (upper panel) and SAM index rower panel) to left-handed (left) and right-handed (right) magnetic clouds; the legend is like in Fig.11.

STRATOSPHERE

To characterize the dynamics of the stratosphere, we use the heat and momentum flux from NCEP reanalysis. The heat and momentum fluxes are indicators of a disturbed stratosphere. The heat flux VT is calculated by correlating the meridional wind and temperature. The heat flux is almost always poleward—positive in the Northern hemisphere and negative in the Southern hemisphere. That is, in the Northern Hemisphere the warm temperatures are transported northward by the merdional wind, while the cold temperatures are transported southward. The momentum flux UV is calculated by correlating the meridional wind and the longitudinal asymmetries of the zonal wind. While the heat flux is almost always poleward, the momentum flux is more variable in direction, but generally also poleward.

Solar flares

Solar flares induce wavy structures in the stratosphere, more pronounced in QBO Easterly phase (Fig. 20 and 21). Enhanced momentum flux and a general increase of the heat flux toward the pole is observed, mainly due to the cases in QBO Easterly, while in QBO Westerly there is an initial decrease followed by a recovery.

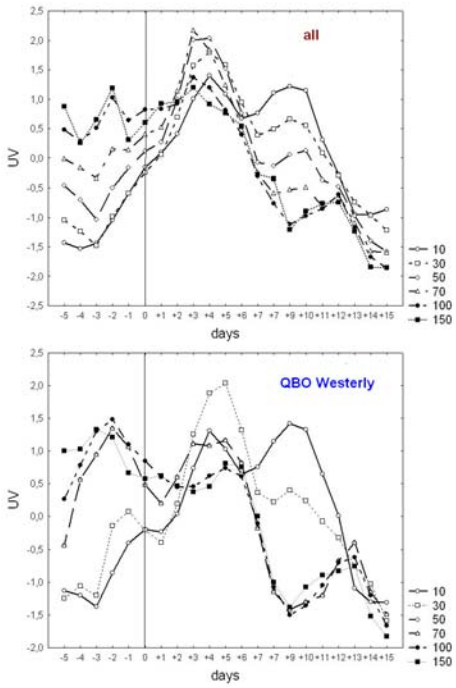

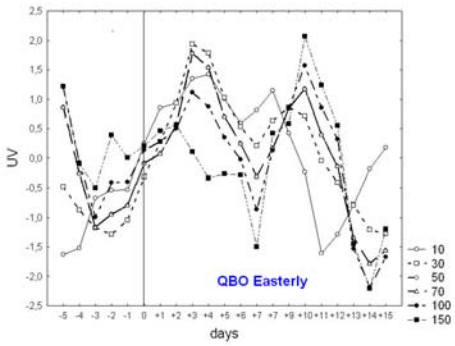

Fig.20. Momentum flux from 10 to 150 hPa after powerful solar flares.

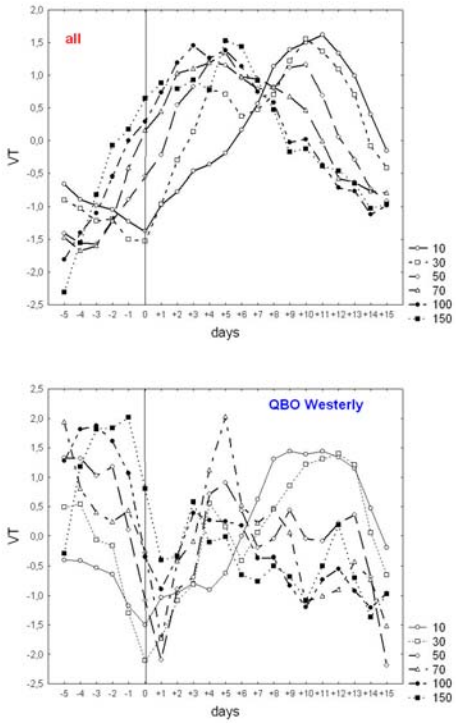

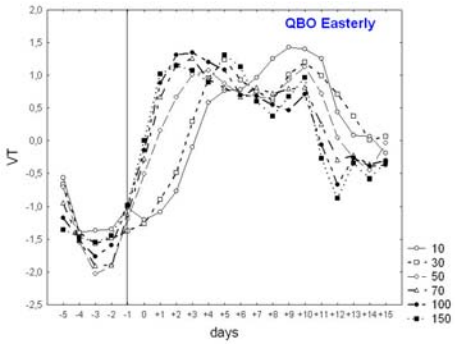

Fig.21. Heat flux from 10 to 150 hPa after powerful solar flares.

High speed solar wind

High speed solar wind also causes waves of heat flux, with a phase difference between QBO Westerly and Easterly phases (Fig.22).

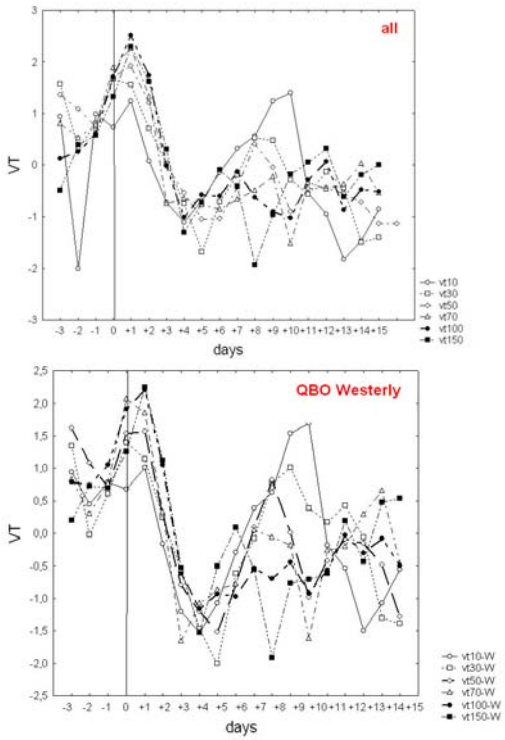

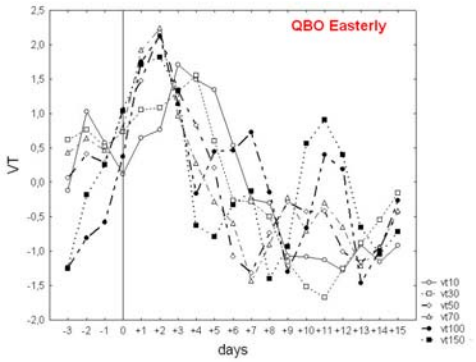

Fig.22. Heat flux from 10 to 150 hPa after high speed solar wind streams.

In the momentum flux, waves in different directions in the lower and upper stratosphere are excited (Brewer-Dobson circulation) – Fig.23. This effect is better expressed in QBO Westerly phase (Fig.24).

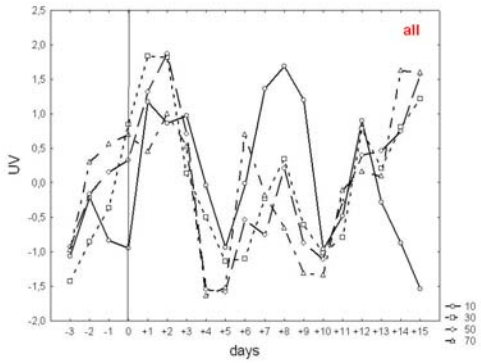

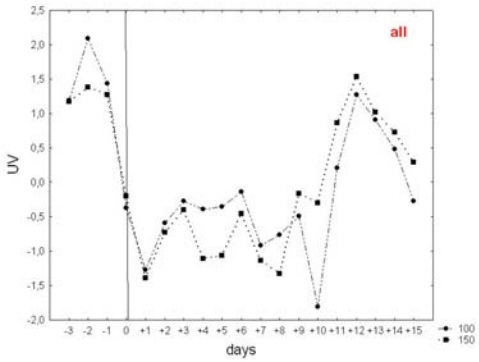

Fig.22. Momentum flux from 10 to 150 hPa after high speed solar wind streams.

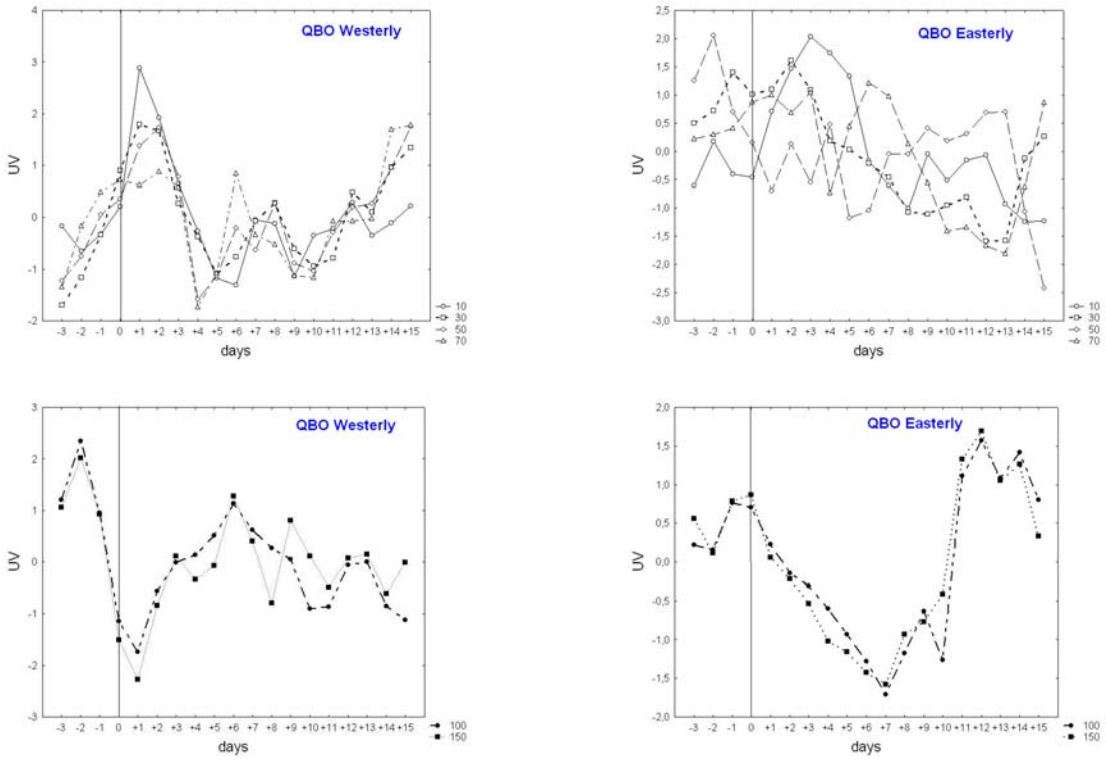

Fig.23. Momentum flux in the upper stratosphere (from 10 to 70 hPa), upper panels, and in the lower stratosphere (100 and 150 hPa), lower panels, after high speed solar wind streams in QBO Westerly phase (left panels) and in QBO Easterly phases (right panels).

Magnetic clouds

The effects of magnetic clouds depend not only on the QBO phase but also on the handedness of the cloud. Left-handed magnetic clouds reduce the momentum flux to the pole, while the right-handed clouds are ambiguous results, and confined to the lower stratosphere (Fig. 24).

The momentum flux decreases and may even turn equatorward in QBO Westerly, while waves in opposite directions in the lower and upper stratosphere are induced in QBO Easterly (Fig. 25).

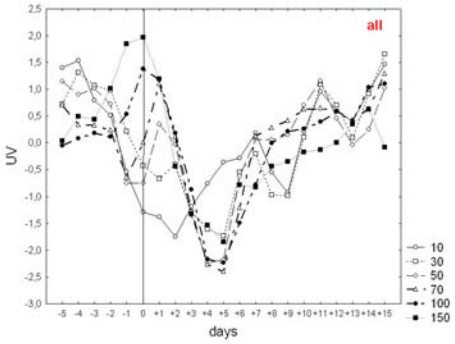

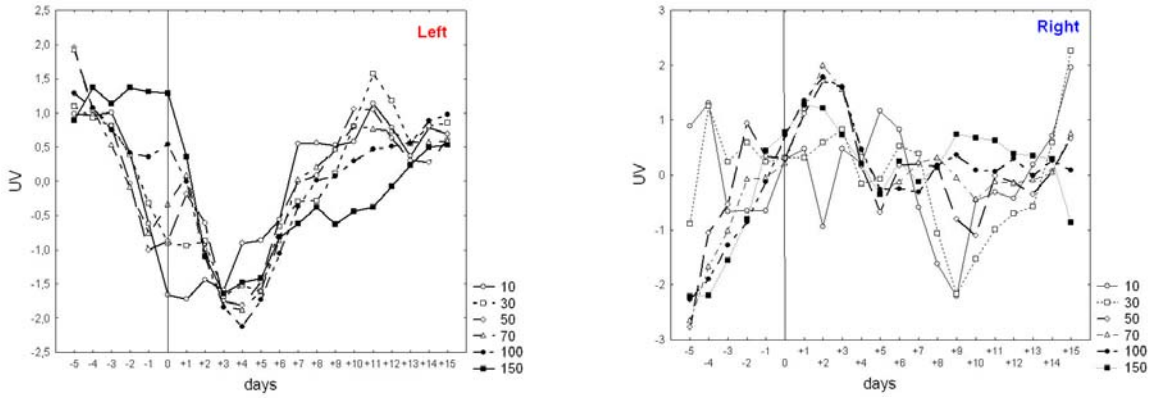

Fig.24. Momentum flux from 10 to 150 hPa after magnetic cloud (upper panel). Lower panel: dependence on the handedness of the clouds – left-handed (left panel) and right-handed (right panel).

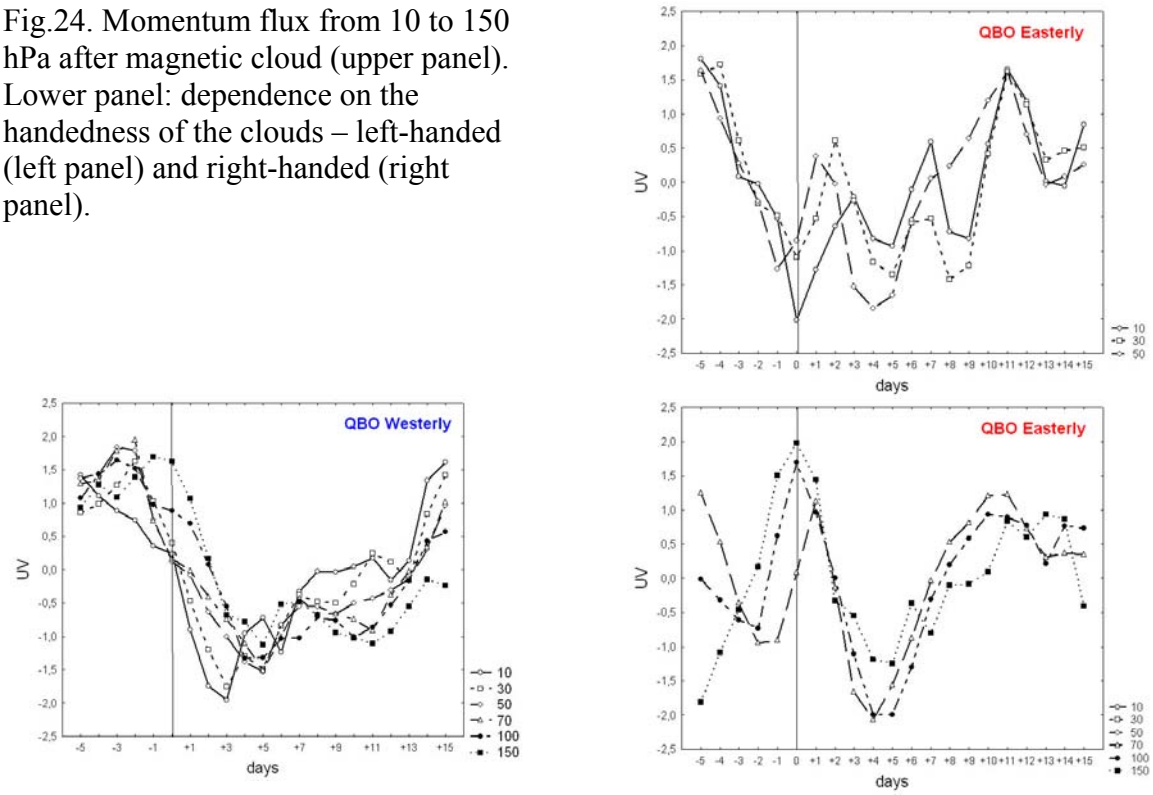

REFERENCES

Antonucci, E., Hoeksema, J.T., Scherrer, P.H., (1990): Rotation of the photospheric magnetic field: a North-South asymmetry. Astrophys. J., 360, 296.

Baldwin, M. P. Annular Modes in Global Daily Surface Pressure. Geophys. Res. Lett. 28, 4115-4118, 2001.

Bartels, J., N. H. Heck, and H. F. Johnston, The three-hour-range index measuring geomagnetic activity, J. Geophys. Res., 44, 411, 1939.

Borovsky, J. E., Denton, M. H. Differences between CME-driven storms and CIR-driven storms. J. Geophys. Res., V. 111, Issue A7, CiteID A07S08, 2006.
Borovsky, J. E., Steinberg, J. T.The ``calm before the storm'' in CIR/magnetosphere interactions: Occurrence statistics, solar wind statistics, and magnetospheric preconditioning. J. Geophys. Res., Vol. 111, Issue A7, CiteID A07S10, 2006.
Borrini, G., Gosling, J. T., Bame, S. J., Feldman, W. C. Helium abundance enhancements in the solar wind, J. Geophys. Res., Vol. 87, 1982, 7370, 1982.
Broussard, R. M., Tousey, R., Underwood, J. H., Sheeley, N. R., Jr. A survey of coronal holes and their solar wind associations throughout sunspot cycle 20. Solar Phys., Vol. 56, 161, 1978.
Feldman, W. C., Asbridge, J. R., Bame, S. J., Gosling, J. T. High-speed solar wind flow parameters at 1 AU. J. Geophys. Res, Vol. 81, 5054, 1976.
Georgieva, K., Kirov, B. Secular cycle of the North-South solar asymmetry, Bulgarian Journal of Physics, Vol.27 No 2,28, 2000.
Gopalswamy, Lara, A., Yashiro, S., Nunes, S., Howard, R. A., In Solar variability as an input to the Earth's environment, ISCS Symposium, 403, 2003.
Gopalswamy, N., Akiyama, S., Yashiro, S., Michalek, G., Lepping R. P. Solar Sources and Geospace Consequences of Interplanetary Magnetic Clouds Observed During Solar Cycle 23. J. Atm. Solar-Terr. Phys. In press, 2007.
Gosling, J. T., Asbridge, J. R., Bame, S. J., Feldman, W. C. Solar wind speed variations - 1962-1974. Journal of Geophysical Research, vol. 81, Oct. 1, 1976, p. 5061-5070.
Hoyt, D.V., Schatten, K.H. Group Sunspot Numbers: A New Solar Activity Reconstruction. Sol. Phys. 181 (2), 491-512, 1998.
Intriligator, D. S.. The solar wind between 0.7 AU and 5.0 AU. In: International Cosmic Ray Conference, 14th, Munich, West Germany, August 15-29, 1975, Conference Papers. Volume 4. (A76-26851 11-93) Munich, Max-Planck-Institut fuer extraterrestrische Physik, 1975, p. 1534-1539, 1975.
Ipavich, F. M., Galvin, A. B., Gloeckler, G., Dovestadt, D., Klecker, B. Solar wind Fe and CNO measurements in high-speed flows. J. Geophys. Res., vol. 91, 4133-4141, 1986.
Jian, L., Russell, C. T., Luhmann, J. G., Skoug, R. M. Properties of Stream Interactions at One AU During 1995-2004. Solar Phys., Vol. 239, Issue 1-2, pp. 337-392, 2006.
Klein, L. W., Burlaga, L. F. Interplanetary magnetic clouds at 1 AU. J. Geophys. Res., vol. 87, Feb. 1, p. 613-624, 1982.
Kumar, A. and Rust, D., (1996): Interplanetary magnetic clouds, helicity conservation, and current-core flux-ropes. J. Geophys. Res., 101 (A7). 15,667.
Luterbacher, J., Schmutz, C., Gyalistras, D., Xoplaki, E., Wanner, H. Reconstruction of monthly NAO and EU indices back to AD 1675. Geophys. Res. Lett., 26 (17), 2745-2748, 1999.
Luterbacher, J., Xoplaki, E., Dietrich, D., Jones, P.D., Davies, T.D., Portis, D., Gonzalez-Rouco, J.F., von Storch, H., Gyalistras, D., Casty, C., Wanner, H., 2001. Extending North Atlantic oscillation reconstructions back to 1500. Atm. Sci. Lett., 2 (2), 114-124, 2001.
Maris, G., Maris, O. High speed plasma streams in solar wind and their geomagnetic effects (III). In: Proceedings of the Second Solar Cycle and Space Weather Euroconference, 24 - 29 September 2001, Vico Equense, Italy. Editor: Huguette

Sawaya-Lacoste. ESA SP-477, Noordwijk: ESA Publications Division, ISBN 92-9092-749-6, 2002, p. 455 – 458

Miralles, M. P., Cranmer, S. R., Kohl, J. L.. Low-latitude coronal holes during solar maximum. Adv. Space Res., Vol. 33, Issue 5, p. 696-700, 2004.

Nindos, A., Andrews, M. D. The Association of Big Flares and Coronal Mass Ejections: What Is the Role of Magnetic Helicity? Astrophys. J., Vol. 616, Issue 2, pp. L175-L178, 2004.

Richardson, I. G., Cane, H. V. Regions of abnormally low proton temperature in the solar wind (1965-1991) and their association with ejecta. J. Geophys. Res., Vol. 100, Issue A12, p. 23397-23412, 1995.

Richardson, I. G., Berdichevsky, D., Desch, D., Farrugia, C. Solar-cycle variation of low density solar wind during more than three solar cycles. Geophys. Rese. Lett., Vol. 27, Issue 23, p. 3761-3764, 2000.

Richardson, I. G., Cane, H. V. The fraction of interplanetary coronal mass ejections that are magnetic clouds: Evidence for a solar cycle variation. Geophys. Res. Lett., Vol. 31, Issue 18, CiteID L1880, 09/2004

Schwenn, R., Rosenbauer, H., Muehlhaeuser, K.-H. Singly-ionized helium in the driver gas of an interplanetary shock wave. Geophys. Res. Lett., vol. 7, Mar. 1980, p. 201-204, 1980.

Sugiura, M., Hourly values of equatorial Dst for IGY, pp. 945-948, in Annals of the International Geophysical Year, vol. 35, Pergamon Press, Oxford, 1964.

Tsurutani, B. T., Lee, Y. T., Gonzalez, W. D., Tang, F. Great magnetic storms.Geophysical Research Letters (ISSN 0094-8276), vol. 19, Jan. 3, p. 73-76, 1992.

Y.-M. Wang, J. Lean, N. R. Sheeley, Jr. The long-term variation of the Sun's open magnetic flux. Geophys. Res. Lett., Vol. 27, No . 4, pp. 505-508, 2000.